CHARACTERIZATION OF THE ASH MELTING PROPERTIES BY VARIOUS BIOMASS ASHES

Raphael Marro*, Karen Friese[1], Andrzej Grzechnik[2], Hartmut Spliethoff [3,4], Matthias Gaderer[4]
[3]Technische Universität München / Institute for Energy Systems / Boltzmannstraße 15, 85747 Garching, Germany
[1]Jülich Center for Neutron Science, Research Center Jülich GmbH, 52425 Jülich, Germany
[2]RWTH Aachen University / Institute of Crystallography
Jägerstr. 17 - 19, 52066 Aachen
[4]ZAE Bayern Abteilung 1, Technik für Energiesysteme und erneuerbare Energien, Walther - Meißner - Str. 6, D- 85748 Garching, Germany
*Corresponding author: Tel.: +49 89 289 16281, Fax: +49 89 289 16271, E-mail:raphael.marro@tum.de

For the high - temperature combustion of biomass, investigations were carried out in an electrically heated entrained flow reactor to analyze the fly ash by varying different parameters. Using torrefied biomass, birch, spruce and straw were used. In general, the main constituents of their ash fractions are K, Si, Ca and Mg, resulting in high alkali indices, which predict a large fouling tendency. We studied the fusibility and flow properties of the bottom ash of the reactor and the laboratory ash. To distinguish the melting behavior of the several ashes, different ex - situ measurement methods were used. The characteristic temperatures, given by the ash melting microscope (AMM), will be compared with the data of differential scanning calorimeter (DSC). Their thermal decomposition properties were studied using thermogravimetric analysis (TGA). With these analyses it was possible to determine and to delimit qualitatively the fusibility of the ash. To characterize the ash composition we used two main techniques: X-ray fluorescence (XRF) to chemically analyze of the samples and X - ray diffraction (XRD) to determine the mineral composition of the samples. Furthermore, chemical equilibrium calculations with the program FactSage were used to understand the nature of the gases, liquids and solids resulting from the biomass combustion. The volume fraction of the liquid and solid phase within a specific temperature range was calculated and will be compared with the data of the AMM and DSC.
Keywords: combustion, reactor, fly ash, torrefied biomass, straw

1 INTRODUCTION

Through the energetic use of biogenic waste materials for heat and power generation, a part of the fossil energy is to be replaced. One way to generate energy can be the combustion of biomass. To increase the use of biomass in the energy sector, for example, residues from agriculture (straw) or short rotation plantations (spruce and birch) can be used. In addition, it is possible to refine the biomass by a torrefaction process. In comparison to the raw fuel, a higher volumetric energy density and a better biological stability are produced by torrefaction. The product of a torrefied biomass is very brittle, which improves the grindability and reduces the associated energy input.

These biogenic fuels are gaining interest related to biomass combustion plants. One possible concept for energy production is shown in Figure 1. Here the biomass is burned at high temperatures. Subsequently, the hot flue gas flows through an air - flow heat exchanger and operates a hot air turbine. Inlet temperatures into the turbine are aimed to be greater than 900 °C. During the combustion, the organic portion of the biomass is converted, whereas the non - combustible inorganic portion of the ash remains. The ash could thus be deposited on the heat exchanger surfaces.

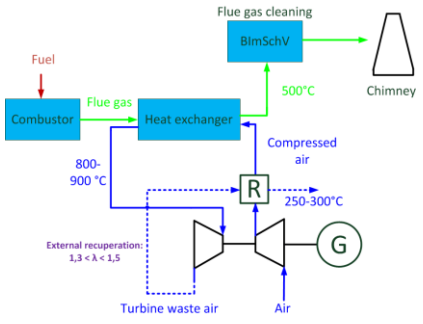

Figure 1: Power generation with a hot - air turbine

Depending on the temperature, the ash can melt, form slag, reduce the heat transport and also the efficiency of the heat exchanger. The uncontrolled deposition of ashes on the heat transfer surfaces can lead to a failure of the system, which is associated with high costs. Depending on the fuel and the combustion temperature, the formation of deposition during combustion can be divided into three types: the contamination with loose deposits, sintering with caking deposits and slagging with molten deposits [1]. The depositions occur mostly in the colder areas of convective heating surfaces. High flue gas velocities lead to inertial deposits of ash particles, which have a low cohesion [1, 2]. The transitional form between fouling and slagging is called sintering. This is not a complete melting phenomenon, but a partial melting of the particles at their surface. This results in a strong cohesion between the particles. Depositions by slagging occur mainly in high temperature regions. The deposits are strongly connected to the chamber wall, around the burners and the radiation field.

In contrast to coal ashes, the melting behavior of biomass ashes has been investigated to a limited extent. A common method of measurement and a certain measuring device is so far not effective. It is rather a combination of different measurement techniques, which are used to analyze the melting behavior.

With the help of the software FactSage, a conclusion on the melting behavior of the ash is made by thermodynamic equilibrium calculations [3, 4]. For example, the calculated phase fractions of the fuel (liquid and solid phase) are compared with the results of the ash melting microscope [5]. Mangialardi investigated the sintering behavior of biogenic fly ashes with DSC and powder diffractometer, where the mineral phases of ash and decomposition reactions could be determined [6]. Hansen et al. addressed, amongst others, the investigation of straw ash by Simultaneous Thermal Analysis (STA) [7]. The results of the STA predictions agree with

predictions of phase diagrams and equilibrium calculations.

2 METHODS / MEASUREMENT TECHNIQUES

2.1 Evaluation Method

To study the ash melting behavior, the following measurement techniques are used. Ash compositions were investigated and determined by X-ray fluorescence (XRF) analysis as well as atomic emission spectroscopy (ICP-OES). Thus, the elemental composition of the ash was determined both qualitatively and quantitatively. To determine the mineral phases, a powder diffractometer (XRD) was used. With the ash melting microscope (AMM), the characteristic melting temperatures could be determined. Due to the rather vague significance of the ash melting microscope, the ashes were measured additionally by Simultaneous Thermal Analysis (STA). The results obtained experimentally were then qualitatively compared and evaluated with equilibrium calculations.

2.2 Ash Treatment

The methods used for the ashing or incineration heat-up and holding periods are the same as DIN EN 14775 or even higher. A holding period of 13 h was chosen to ensure a full implementation of larger sample volumes during incineration.

2.3 XRF Measurements

For ash analysis, the instrument of Shimadzu EDX-800 HS was used. The examination requirement for fuel ashes by means of compressed tablets according to DIN 14775 for the determination of ash composition was used in this case. The pellet contains 100 mg of the test ash and 20 mg of a binder, in this case wax. The mixing ratio should always be 10:2. After successfully weighing the material mixture, it has to be mixed for 3 minutes in an agate mortar to homogenize and then filled in a pressed mold.

2.4 ICP – OES Measurements

With the help of a suitable flux (lithium metaborate), the biomass according to DIN 51729 is manufactured according to DIN EN 14775 - 11. The sample was mixed with lithium metaborate $LiBO_2$ and melted at 1050 °C for about 15 min. After cooling, the melt is dissolved by hydrochloric acid (HCl). Only clear fusion solutions should be used for the investigation of the ICP - OES.

2.5 XRD Measurements

Powder X - ray measurements were performed at room temperature using the diffractometer X'Pert (Philips) in a Bragg-Brentano geometry with the Cu-Kα radiation. The phase identification was carried out using the software HighscorePlus2.2.2 (Panalytical) and PowderCell 2.4 *[W. Kraus & G. Nolze, Federal Institute for Materials Research and Testing, Berlin, Germany]* in a combination with the Inorganic Crystal Structure Database (Karlsruhe, Germany). Semi-quantitative analysis of the detected phases was performed with the software Powdercell.

2.6 AMM Measurements

The melting microscope used is by the company Hesse Instruments. Due to the fact that the investigation of the ash melting behavior by ASM is an optical measuring method, according to DIN CEN / TS 51730 - 1 convention we need to define factors to determine the characteristic temperatures for biomass more precisely. For the tests, a cylindrical specimen was prepared. The measurement was repeated at high deviations to the determined values i.e > 30 °C. All experiments were carried out under atmospheric conditions.

2.7 STA Measurements

Coupling a thermo balance type STA PT1600 by the company Linseis with a DSC sample holder creates the TG - DSC instrument (STA) with which it is possible to draw conclusions on both chemical decomposition reactions as well as on the ash melting behavior. In this simultaneous measurement technique we detect the change in mass due to temperature dependence and in addition to this we can detect simultaneously the endothermic and exothermic heat flows. For evaluation the software TA Evaluation V 2.0.0 by Linseis was used. The Al_2O_3 crucible had the following dimensions: outer diameter 7 mm, height 4 mm and wall thickness 0.5 mm. The STA samples to be investigated were prepared in accordance with DIN 51006. For better comparability of the results always the same initial weight (about 15.75 mg) was used, with a specially designed plunger that compresses the ash in the crucible and spread evenly. All experiments were carried out under oxidizing conditions. Here, the reaction chamber of the instrument was flushed with 100 nml / min.

2.7 FactSage Modeling

The calculation program FactSage was used for the simulation of equilibrium calculations. The calculation method is based on the Gibbs energy minimization, with less than 0.01 wt.% phases neglected. As a basis for the calculations both the organic and the inorganic constituents of the fuel are used in the form of pure elements. The organic constituents were determined according to DIN 51721 up to DIN 51727 on the basis of elemental analysis (MACRO-Company for elemental analysis systems GmbH). The inorganic components were determined by XRF. Here, the fuels were ashed at 550 °C. The air ratios required for the experiments were taken into account and implemented into FactSage. The databases used were FT-oxide, FT-Salt and FACT-PS. The expected mixed crystals were estimated by appropriate phase diagrams. As a result, the composition of the gas, solid and liquid phase of individual fuels was generated. Furthermore, the phase fractions (solid - liquid) are determined as a function of temperature and air speed.

3 RESULTS

To investigate the melting behavior of the ash, these feedstocks are first combusted in a muffle furnace at different temperatures. On the one hand torrefied wood (spruce, birch, alder, poplar) and straw (wheat and triticale) ashes have been studied. Because of the similar behavior (composition, melting behavior) of the woody biomass but also of the straw only the results of birch on the woody and wheat straw on the herbaceous site are shown in this contribution.

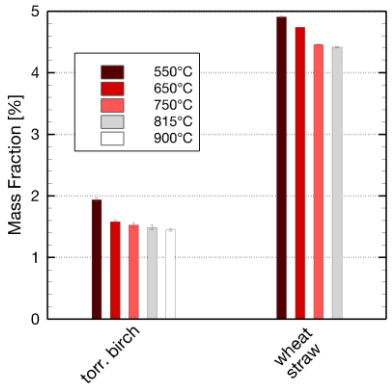

Figure 2: Ash content of torrefied birch and wheat straw at different ashing temperatures

In Figure 2 the typical ash content of woody and herbaceous biomass is shown. The higher incineration temperature reduces the mass of birch ash from 550 to 900 °C to nearly 26 wt.%, the straw ash by almost 11 wt.%. This is due to the evaporation of alkali, the oxidation of carbon but also due to decomposition reactions. The incineration of straw at 900 °C led to a caking of the ash with the aluminum pan, so that no measurement was possible here.

3.1 Wheat straw ash

The three main components of the straw ash are SiO_2, K_2O and CaO. The combustion temperatures are color coded. The ashing apparently has no major influence on the composition of the straw ash (Figure 3). The low SiO_2 content at 650 and 750 °C is due to possible matrix effects and measurement inaccuracies.

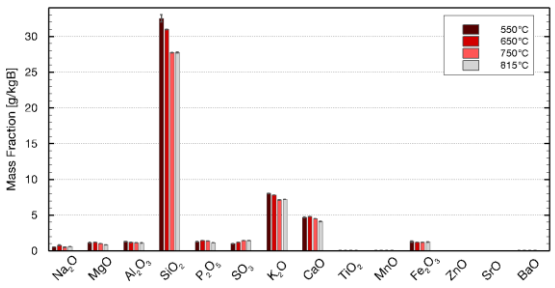

Figure 3: Composition of wheat straw ash

The assumption can be further supported by the STA study. Straw ash was produced in the experiments presented in Figure 4 at a heating rate of 10 K / min. The TG measuring curve appears to undergo a steady decrease in mass at all ashing temperatures. On closer consideration, however the ash scales are very fine. This falsely gives the impression that the total mass loss resembles the decrease of the torrefied biomass (see Figure 6). The thermal decomposition reactions over the entire temperature range result for a 550 °C ash in a mass reduction of 1.3 mg. This is one third of the thermally decomposed mass compared to torr. birch. Due to the difference in buoyancy between zero and sample measurement curve, the slope of the curve slightly decreases. The fact that these are not decomposition reactions is shown by the dm / dT - measurement curve. Until there is a slight deflection/change in the 550 °C ash, the curve can be described horizontally. As long as the values remain approximately constant, the decreasing TG measurement curve can be explained by said buoyancy differences. The signal noise of the Delta MId curve in the upper temperature range indicates the slow melting or swelling of the straw ash. The shrinkage temperatures A and flow temperatures D, which are referred in addition to the softening as well as the hemisphere temperature, also called characteristic temperatures, are shown in Figure 4. The temperatures with the letters are used to denote the ashing or incineration temperatures. Thereby, during heating the characteristic melting temperatures are determined by the optical change of the sample surface by means of the ASM while no phase change may be detected within the sample by this measurement method. When comparing the shrinkage temperatures with the signals of the Delta MId curve, a beginning of noise is recognizable at the corresponding temperatures. Furthermore, the curve between the shrinkage and flow temperature drops. This drop is partly given by the furnace geometry. However, previous attempts to baseline determination have found out that when inert samples (SiO_2) are heated, the curve does not fall to such an extent in the temperature range of 950 - 1200 °C. Excluding the 815 °C ash, the characteristic temperatures increase with higher ashing temperatures.

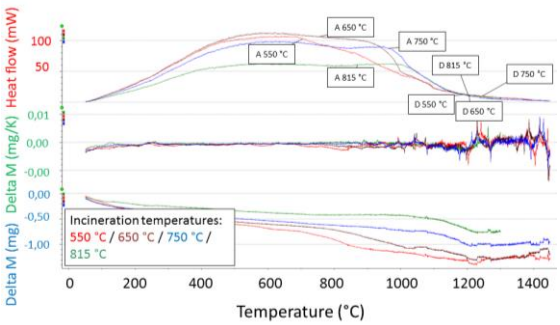

Figure 4: STA curve of wheat straw

3.2 Torrefied birch

The ash composition of the torrefied birch is illustrated in Figure 5. In contrast to the straw a higher ashing temperature of 900° C was chosen. The three main components are characterized by the thermal stability of CaO and SiO_2 as well as the thermal decomposition of K_2O.

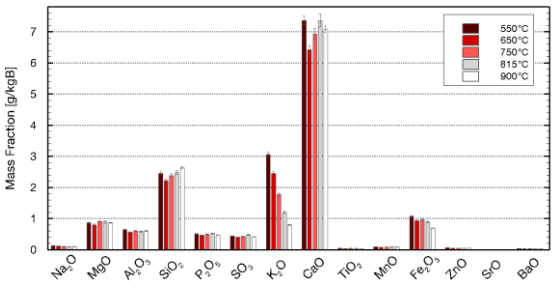

Figure 5: Composition of torrefied birch

Noticeable in this context are the decrease of K_2O and the increase of CaO content. It is assumed that the increase of CaO at 900 °C is caused by matrix effects. Measurements with the powder diffractometer have shown that the ash (incineration at 550 °C) leads to 44.1 wt.% of calcite and

17.6 wt.% of fairchildite. In a temperature range between 550 and 870 °C, the decomposition of calcite and fairchildite to CaO in woody biomass was found by Porbatzki [8]. Through the production of calcium as an oxide the XRF measurement could be affected.
Comparing the STA results of the torr. birch from Figure 6 with those of straw, the peaks fall directly in the low to mid temperature range. The first peak of the sample in the temperature range 360 - 420 °C are attributed to the vaporization of crystal water and the decomposition of the alkaline earth metals (Ca, Mg). This evaporation is detected on the one hand through an endothermic change in the heat flow signal and on the other hand by a slight decrease in mass (dm = 0.3 mg). As expected, the endothermic decomposition reaction decreases with increasing combustion temperature. The temperature range 600 - 800 °C is highlighted. Here the mass change of the 550 °C ash is 3.5 mg, while for the 650 °C ash it is only 1 mg. It can be concluded that the majority of decomposition reactions take place between these ashing stages. We assume the following decomposition reactions [9] [10] [11]:

$$CaCO_3\,(s) \rightarrow CaO\,(s) + CO_2\,(g)$$
$$MgCo_3\,(s) \rightarrow MgO\,(s) + CO_2\,(g)$$
$$K_2CO_3\,(s) \rightarrow K_2O\,(s) + CO_2\,(g)$$

Furthermore, it is assumed that evaporation of potassium compounds is in this temperature range. This assumption can be supported by both the XRF measurements in Figure 5 as well as by equilibrium calculations with FactSage. A further mass loss occurs during the melting process (about T > 1300 °C). This is subject to any ashing stage of a similar mass reduction of approximately 0.5 mg. On the basis of the dm/dT measurement curve, it can be seen that all the corresponding thermal decomposition reactions of different birch ashes start simultaneously from a temperature of 550 °C. Only the characteristic of the peaks decreases with increasing temperature. This is accompanied by a shift of the temperature of the maximum reaction volumes to lower temperatures. The mass decrease in the temperature range from 550 °C to 850 °C for ashing temperatures of 550 °C and 650 °C appears to consist of two different reactions, which is also reflected in the DSC curve. A closer look at the melting range shows a lower dependence of the melting process from the ashing temperature for birch in comparison to spruce. Here, the melting peaks change slightly from 550 °C ashes to 815 °C ashes and have an easily identifiable peak. The 900 °C ash, however, shows only several small peaks. There is no clear trend visible with respect to the shrinkage temperatures (A) and flow temperatures (D). However, what we can see in all measurements is that the delta M signal curve starts to be noisy just before the respective shrinkage temperature. Except for the 900 °C ash, the melting peak in the heat flow diagram in Figure 6 sets in before the flow temperature detection with the AMM.

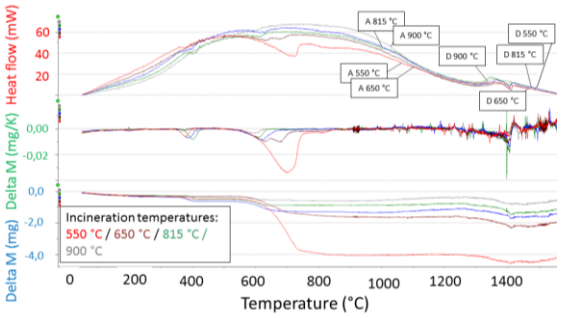

Figure 6: STA curve of torrefied birch

3.3 FactSage

In Figure 7, the combustion of birch and in Figure 8 the combustion of straw are shown using equilibrium calculations. The letters A and D identify again the shrinkage temperature and the flow temperature which were determined by the ash melting microscope. In this diagram, the liquid and solid fractions are shown as a function of temperature. Measurements of different samples have shown that the shrinkage temperature always appears in a calculated liquid phase content of around 15 – 30 wt.%. The liquid phase region is indicated by two dashed lines. Furthermore, it was found that the flow temperature corresponds approximately to a liquid phase content of 75 – 80 wt.%.

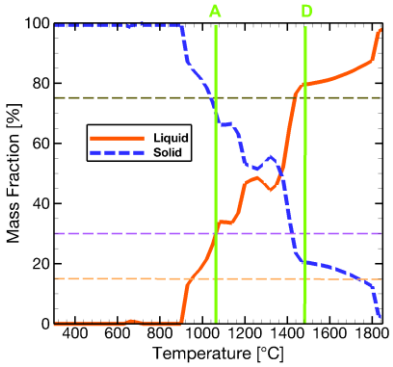

Figure 7: Simulation of combustion with torr. birch

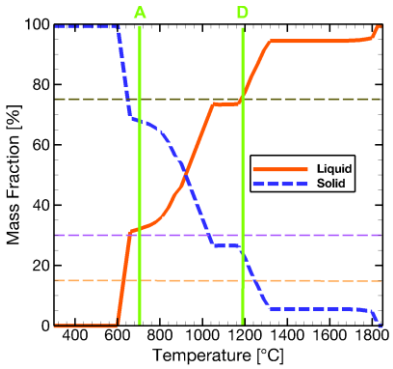

Figure 8: Simulation of combustion with wheat straw

3.3 Comparison between reactor and laboratory ash (torr. birch)

The fly and bottom ash, which was produced during the combustion of torrefied birch at a temperature of 1400 °C and an air ratio of 1,13 were analysed with the STA (see Figure 9). The reason for the exothermic peak of the heat flow in the temperature range of 300 – 500 °C is because of the remaining carbon in the ash and the oxidation to CO_2 during the heating. The burnout of the fly ash is 97.5 %, that of the bottom ash 69 %. The fuel has the average particle size of 150 µm whereat 95 % of the ash remained as fly ash in the cyclone separator so that the bottom ash can is negligible.

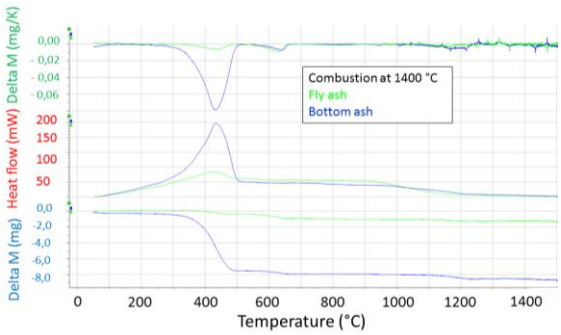

Figure 9: STA analysis of fly and bottom ash of torr. birch

In contrast to the laboratory ashes of birch, in the fly and bottom ash, no characteristic melting peaks could be identified.

3.4 Correlation of the data

In accordance with Obernberger in Figure 10 for a characterization of the ash melting behavior the shrinkage temperature against the (Si + P + K) / (Ca + Mg) ratio is plotted [12].

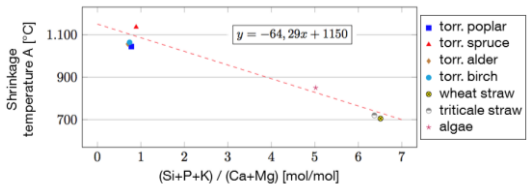

Figure 10: Correlation between the shrinkage temperature and the alkali content

Figure 10 shows that with an increasing Si, P, or K-content the ash fusion temperatures decrease and increase with a higher content of Ca or Mg. Between the studied biomass is actually an approximately linear relationship, as the curve shows. Using this correlation, an approximate estimation of the determined (Si + P + K) / (Ca + Mg) ratio on the shrinkage temperature can be taken but also the reverse approach is possible.

4 DISCUSSION

In order to characterize the melting behavior of ash, a combination of different measurement techniques must be used. The characteristic temperatures (A, D) of the ash melting microscope are in good agreement with the equilibrium calculations and STA results. The characteristic signal of the beginning of the melting or of the melt flow occurs earlier in the STA curve, i.e. at lower temperatures in comparison to the ash melting microscope. Comparing the STA values of straw with that of torr. birch, for straw neither a higher mass loss nor a melting peak is detected. This behavior is confirmed by the XRF data up to a temperature of 900 °C as each element at different ashing temperature levels remains almost constant (see Figure 2). The composition of the straw ash appears to remain unchanged despite heating.

Unlike for straw, strong decomposition reactions take place for the torr. birch, which can be understood partially by the XRF data shown in Figure 5. In addition, here a characteristic melting peak is visible. This peak was also observed for the torr. spruce. Measurements of both woody and herbaceous biomass have shown that the corresponding shrinkage temperatures are always in a liquid phase content of 15 - 30 wt.% (see Figure 7/8). The flow temperature D is in a liquid phase content of 75 – 80 wt.%.

Furthermore a correlation between the alkali content and the shrinkage temperature of various biomasses was found. This Knowledge has to be verified by more biomasses to give a reliable declaration for a norm.

6 REFERENCES

[1] Muhammadieh M. Beitrag zur Ermittlung des Ansatzbildungspotenzials von Braunkohlen in Dampferzeugern: Technische Universitaet Bergakademie Freiberg Universitaetsbibliothek "Georgius Agricola"; 2009.

[2] Spliethoff. Prozesstechnik und Umweltschutz in modernen Kraftwerken. München; 2012.

[3] Berjonneau J, Colombel L, Poirier J, Pichavant M, Defoort F, Seiler J. Determination of the Liquidus Temperatures of Ashes from the Biomass Gazification for Fuel Production by Thermodynamical and Experimental Approaches. Energy Fuels 2009;23(12):6231–41.

[4] Evic N, Brunner T, Obernberger I. Prediction of biomass ash melting behaviour - correlation between the data obtained from thermodynamic equilibrium calculations and simultaneous thermal analysis (STA). In: Proceedings of the 20th European Biomass Conference & Exhibition; 2012, p. 807–813.

[5] Wieland C, Kreutzkam B, Balan G, Spliethoff H. Evaluation, comparison and validation of deposition criteria for numerical simulation of slagging. (1) Green Energy; (2)Special Section from papers presented at the 2nd International Enery 2030 Conf 2012;93(0):184–92.

[6] Mangialardi T. Sintering of MSW fly ash for reuse as a concrete aggregate. Journal of Hazardous Materials 2001;87(1–3):225–39.

[7] Hansen LA, Frandsen FJ, Dam-Johansen K, Henning Sund Sørensen. Quantification of fusion in ashes from solid fuel combustion. Thermochimica Acta 1999;326(1–2):105–17.

[8] Porbatzki D. Freisetzung anorganischer Spezies bei der thermochemischen Umwandlung biogener Festbrennstoffe. Dissertation. Aachen; 2008.

[9] Liodakis S, Katsigiannis G, Kakali G. Ash properties of some dominant Greek forest species.

Thermochimica Acta 2005;437(1–2):158–67.
[10] Kirnbauer F, Koch M, Koch R, Aichernig C, Hofbauer H. Behavior of Inorganic Matter in a Dual Fluidized Steam Gasification Plant. Energy Fuels 2013;27(6):3316–31.
[11] Olanders B, Steenari B. Characterization of ashes from wood and straw. Biomass and Bioenergy 1995;8(2):105–15.
[12] Ingwald Obernberger. Strategy for the Application of Novel Characterisation Methods for Biomass Fuels - Case Study Straw. Energy Fuels 2014.

6 ACKNOWLEDGEMENTS

The financial support from the Federal Ministry of Food and Agriculture (FKZ: 22023911) is gratefully acknowledged. The authors also like to thank all students of TUM, who work on this project.